HHS Public Access

Author manuscript

J Thromb Haemost. Author manuscript; available in PMC 2020 May 01.

Published in final edited form as:

J Thromb Haemost. 2019 May ; 17(5): 737–748. doi:10.1111/jth.14412.

Factor XIII topology: organization of B subunits and changes with activation studied with single-molecule atomic force microscopy

ANNA D. PROTOPOPOVA[*], **ANDREA RAMIREZ**[*,†], **DMITRY V. KLINOV**[‡], **RUSTEM I. LITVINOV**[*,§], **JOHN W. WEISEL**[*]

[*]Department of Cell and Developmental Biology, University of Pennsylvania School of Medicine, Philadelphia, PA;

[†]Border Biomedical Research Center, Department of Biological Sciences, University of Texas at El Paso, El Paso, TX, USA;

[‡]Federal Research and Clinical Center of Physical-Chemical Medicine, Moscow;

[§]Institute of Fundamental Medicine and Biology, Kazan Federal University, Kazan, Russian Federation

Summary.

Background: Factor XIII (FXIII) is a precursor of the blood plasma transglutaminase (FXIIIa) that is generated by thrombin and Ca^{2+} and covalently cross-links fibrin to strengthen blood clots. Inactive plasma FXIII is a heterotetramer with two catalytic A subunits and two non-catalytic B subunits. Inactive A subunits have been characterized crystallographically, whereas the atomic structure of the entire FXIII and B subunits is unknown and the oligomerization state of activated A subunits remains controversial.

Objectives: Our goal was to characterize the (sub)molecular structure of inactive FXIII and changes upon activation.

Methods: Plasma FXIII, non-activated or activated with thrombin and Ca^{2+}, was studied by single-molecule atomic force microscopy. Additionally, recombinant separate A and B subunits were visualized and compared with their conformations and dimensions in FXIII and FXIIIa.

Results and Conclusions: We showed that heterotetrameric FXIII forms a globule composed of two catalytic A subunits with two flexible strands comprising individual non-catalytic B subunits that protrude on one side of the globule. Each strand corresponds to seven to eight out of

Correspondence: John W. Weisel, room 1154, BRB II/III, 421 Curie, Boulevard, Philadelphia, PA 19104-6058, USA, Tel.: +1 215 898 3573, weisel@pennmedicine.upenn.edu.

Addendum

A. D. Protopopova concept and design, acquisition, analysis and interpretation of data, and writing. A. Ramirez acquisition, analysis and interpretation of data. D. V. Klinov provided critical methodology. R. I. Litvinov concept and design, interpretation of data, and writing. J. W. Weisel concept and design, interpretation of data, and writing. All authors approved the final version to be published.

Disclosure of Conflict of Interests

The authors declare that they have no conflict of interests with the contents of this article.

Supporting Information

Additional supporting information may be found online in the Supporting Information section at the end of the article:

10 tandem repeats building each B subunit, called sushi domains. The remainder were not seen, presumably because they were tightly bound to the globular A_2 dimer. Some FXIII molecules had one or no visible strands, suggesting dissociation of the B subunits from the globular core. After activation of FXIII with thrombin and Ca^{2+}, B subunits dissociated and formed B_2 homodimers, whereas the activated globular A subunits dissociated into monomers. These results characterize the molecular organization of FXIII and changes with activation.

Keywords

atomic force microscopy; blood; blood coagulation factor; factor XIII; transglutaminases

Introduction

Blood coagulation factor XIII (FXIII) is the precursor of transglutaminase (FXIIIa) that covalently crosslinks fibrin and other plasma proteins. FXIIIa catalyzes formation of an isopeptide bond between the γ-carboxy-amide group of a glutamine residue and the ε-amino group of a lysine residue in adjacent molecules. Fibrin crosslinking by plasma FXIIIa increases stiffness of individual fibrin fibers [1–3] and the whole clot fibrin network [4–8], changes the extensibility of fibrin fibers [1,2], compacts protofibrils within a fibrin fiber [9] and changes the overall fibrin clot structure [6]; it also prevents red blood cell fallout from clots [10,11] and affects platelet-driven clot contraction [12–17]. FXIIIa-catalyzed incorporation of fibrinolysis inhibitors into fibrin increases its proteolytic stability [18–21]. In summary, FXIIIa-catalyzed crosslinking is crucial for the lytic and mechanical stability of blood clots and congenital FXIII deficiency is associated with bleeding disorders [22].

Structurally, inactive plasma FXIII is a 326-kDa heterotetramer (A_2B_2) with two 83-kDa catalytic A subunits (FXIII-A) and two non-catalytic 80-kDa B subunits (FXIII-B) [23–25]. Besides plasma FXIII (pFXIII), there is a cellular form of FXIII (cFXIII) composed of two A subunits without B subunits (FXIII-A_2) [23–25]. cFXIII is present in platelets, megakaryocytes, monocytes and macrophages and has been shown to play a role in hemostasis, wound healing, angiogenesis, maintaining pregnancy, etc. [23,26,27].

In (patho)physiological conditions, the inactive pFXIII is converted into a catalytically active form (pFXIIIa) by thrombin and Ca^{2+} in two steps [28]. First, thrombin cleaves off a 37-residue-long activation peptide (AP) from the N-terminus of each A subunit, rendering them to the potentially active intermediate form (A'):

$$A_2B_2 \xrightarrow{\text{Thr}} A'_2B_2 + 2AP \quad (1)$$

Next, in the presence of Ca^{2+} the inhibitory B subunits dissociate from the intermediate inactive complex A'_2B_2, resulting in formation of the active pXIIIa-A^*_2:

$$A'_2B_2 \xrightarrow{Ca^{2+}} A^*_2 + B_2 \quad (2)$$

Equations (1) and (2) could be summarized as follows:

$$A_2B_2 \xrightarrow{\text{Thr, } Ca^{2+}} A_2^* + B_2 + 2AP \quad (3)$$

Equation (3) reflects a commonly accepted notion that the active form of pFXIIIa is a dimer of the A* subunits (A^*_2) [29–31]. However, in contrast to the existing paradigm, a recent study has suggested that during activation of FXIII-A_2 the complex dissociates into monomers (A*) [32]. Despite being at variance with biochemical studies [29,31], this idea is in line with the monomeric crystal structure of activated cFXIIIa [33] and with molecular dynamics simulations, suggesting weakening of the A : A inter-subunit interface after activation of pFXIII [34]. Thus, whether the active FXIIIa is dimeric (FXIII-A^*_2) or monomeric (FXIII-A*) has been a matter of controversy.

Cellular FXIII (cFXIII-A_2) can be activated with thrombin and Ca^{2+} as pFXIII-A_2B_2, but it can also be slowly activated by Ca^{2+} without proteolysis [35]. Crystallographically, the inactive cFXIII comprises an A_2 dimer with a cylinder-like structure [36–38], whereas the non-proteolytically activated cFXIIIa in complex with a covalently bound inhibitor existed as an A monomer undergoing conformational rearrangement upon activation to expose the catalytic center [33].

Unlike isolated A subunits, the atomic structures of the heteromeric pFXIII-A_2B_2 complex and isolated B subunits remain unknown. The B subunit of pFXIII is a glycoprotein consisting of 10 tandem repeats, called “sushi domains”, each containing about 60 amino acid residues held together by disulfide bonds. Low-resolution structural data on FXIII-B and full pFXIII-A_2B_2 were obtained using transmission electron microscopy [39]. Isolated B subunits appeared as thin, flexible ~30-nm-long and 2–3-nm-thick strands. Based on sedimentation analysis, these B subunits were suggested to exist as monomers; however, this assumption contradicts other evidence [29,40]. Electron microscopy of glutaraldehyde-crosslinked pFXIII-A_2B_2 (but not uncrosslinked pFXIII-A_2B_2) revealed asymmetric globular particles, in which individual subunits were not discernible. Based on these data, B subunits of pFXIII-A_2B_2 are thought to be tightly wrapped around the globular core formed by the A_2 dimer. Unfortunately, the biophysical studies of reversibly denatured pFXIII did not reveal details of the subunit assembly in pFXIII-A_2B_2 [41–43]. Therefore, the structure of individual pFXIII-B subunits and their topology in the pFXIII-A_2B_2 tetramer remain largely unknown.

Here, we visualized and characterized quantitatively the morphology of the entire pFXIII-A_2B_2 molecules and individual A and B subunits before and after proteolytic activation using high-resolution single-molecule atomic force microscopy (AFM) [44,45]. We showed that pFXIII consisted of a globular A_2 dimer and thin flexible strands of B subunits that typically protrude from the globular core. In activated pFXIIIa, the B subunits dissociated from the A_2 globules and existed as B_2 dimers, whereas the dimeric A_2 globules fell apart into catalytically active A* monomers.

Materials and methods

Preparations of plasma-purified (pFXIII) and recombinant (rFXIII) human factor XIII

pFXIII and pFXIIIa were purchased from Enzyme Research Laboratories (South Bend, IN, USA). The inactive pFXIII was > 94% pure in SDS-PAGE (Fig. 1A) with a potential 2950 Loewy U mg^{-1} specific transglutaminase activity (1 Loewy U mL^{-1} is defined as the highest dilution of the enzyme capable of forming an insoluble clot under the conditions described in [46]). Preactivated pFXIIIa was > 94% pure (Fig. 1A) and had a specific activity of 2778 Loewy U mg^{-1}. In addition, we used: (i) inactive rFXIII-A subunits from ZymoGenetics (Seattle, WA, USA), > 95% pure (Fig. 1A) with a potential 3049 Loewy U mg^{-1} specific activity; (ii) inactive rFXIII-A subunits from Zedira (Darmstadt, Germany), > 95% pure (Fig. 1A) with a potential 3343 Loewy U mg^{-1} specific activity (the latter preparation contained maltodextrin as a stabilizer, which formed a non-uniform background in AFM images; see Fig. S2); and (iii) inactive rFXIII-B subunits from Zedira, > 95% pure (Fig. 1A).

Subunit composition of the FXIII preparations was evaluated by 7.5% SDS-PAGE (Fig. 1A) in Laemmli buffer [47]. In reducing SDS-PAGE, the A and B subunits were overlapping, as has been shown before [24], and separated only after partial cleavage of the A subunits with thrombin because activated FXIII-A* became 4-kDa smaller and appeared as a separate band (Fig. 1B); A* and B subunits were initially separated in the commercially available preactivated pFXIIIa (Fig. 1A). In non-reducing conditions, the A and B subunits of inactive pFXIII were revealed as clearly separated bands (Fig. 1A, insert); some degree of heterogeneity of FXIII-A subunits seen in non-reducing conditions is probably a result of partial cleavage or glycosylation [48]. Composition of the two preparations of rFXIII-A subunits (from ZymoGenetics and Zedira) were similar to each other and identical to the A subunits of pFXIII. rFXIII-B subunits had smaller molecular weight than their plasma-purified counterparts because of a different glycosylation pattern (Fig. 1A).

Activation of FXIII with thrombin and Ca^{2+}

pFXIII or rFXIII-A_2 were diluted to a 0.267 mg mL^{-1} concentration with 20 mM HEPES buffer, pH 7.4, containing 150 mM NaCl and 5 mM $CaCl_2$. Human thrombin (T4393, Sigma-Aldrich, St. Louis, MO, USA) was added at a final concentration of 0.4 NIH U mL^{-1} and the mixture was incubated for 10 min, 30 min, 2 h or 3 h at 37 °C. In 2 h pFXIII was fully activated by the partial cleavage, as determined by the conversion of the A subunits to the smaller A* subunits (Fig. 1B). Cleavage of rFXIII-A subunits from ZymoGenetics was slower and was almost complete in 3 h (Fig. 1C). The same results were obtained with rFXIII-A subunits from Zedira (Fig. S1). At 30 min after addition of thrombin, about half of the A subunits of both pFXIII and rFXIII-A_2 were partially cleaved to the activated state (Fig. 1B–C). We used 5 mM $CaCl_2$, which can potentially induce very slow non-proteolytic activation of FXIII that would not exceed 1% at 30 min [49], so our AFM images should not detect non-proteolytic activation of FXIII.

The BioVision Colorimetric FXIIIa Activity Assay Kit (BioVision, Milpitas, CA, USA) was used to determine specific transglutaminase activity of activated FXIII preparations normalized by the protein concentration determined at λ = 280 nm, assuming $A_{lcm}^{0.1\%} = 1.49$

for rFXIII-A and $A_{1cm}^{0.1\%}$ = 1.38 for pFXIII [32,50]. The activity assay utilizes the transglutaminase activity of FXIIIa to crosslink an amine-containing substrate to a glutamine-containing substrate, resulting in the release of the ammonium cation, which is quantified with a detection reagent that has a decreased absorbance at 340 nm upon reaction with $NH4^+$.

Sample preparation for AFM

Preparations of FXIII and its derivatives were diluted to 2 μg mL^{-1} with 20 mM HEPES buffer, pH 7.4, containing 150 mM NaCl and 5 mM $CaCl_2$. Typically 2 μL of the diluted protein solution was applied on a substrate and kept for 5–15 s. Then 200 μl of fresh milli-Q water was carefully placed over the sample, kept for 10 s and removed with a flow of air to dry the surface. All the protein samples were adsorbed on the highly oriented pyrolytic graphite coated with an amphiphilic graphite modifier (GM-graphite), used earlier for high-resolution single-molecule AFM imaging of proteins and nucleic acids [44,45,51].

Acquisition and processing of AFM images

AFM imaging was performed using a MFP-3D microscope (Asylum Research, Goleta, CA, USA) in a tapping mode with a typical scan rate of 0.5 Hz. Images were taken in air using sharpened silicon cantilevers, SSS-SEIHR (Nanosensors, Neuchâtel, Switzerland), with guaranteed tip radius < 5 nm or standard cantilevers, OMCL-AC200TS (Olympus, Tokyo, Japan), with a typical tip radius of 7 nm. FemtoScan Online software (http://www.femtoscanonline.com) was used to filter, analyze and present the AFM images. SPM Image Magic software (https://sites.google.com/site/spmimagemagic) was used for a semi-automatic measurement of the height of visualized objects.

Statistical analysis

Statistical analysis was performed in R (https://www.r-project.org) using the package Psych (https://cran.r-project.org/web/packages/psych). The results are presented as mean ± SD.

Results

Molecular structure of inactive FXIII and its subunits

Structure of tetrameric pFXIII-A_2B_2—Individual molecules of pFXIII adsorbed on a GM-graphite surface were visualized in AFM as a globule with two, one or no thread-like extensions (Fig. 2A,B). Two strands (typically, both on one side of the globule) were seen in 67% of the molecules, one in 14%, and no strands were seen in 19% of the pFXIII-A_2B_2 molecules (n = 418). The size (height) of the globular portions had a symmetrical distribution with a maximum at 3.5 ± 0.5 nm (n = 2511, Fig. 2C). The shape of the globular portion of pFXIII was characterized quantitatively using circularity (i.e. the ratio of the projected area of an object to an area of a circle with the same perimeter; the circularity of a circle is equal to one, whereas for elongated structures it is smaller). We measured the perimeter and area of projections of 40 randomly selected globular cores of pFXIII molecules with two visible extensions. The calculated average circularity was equal to 0.86 ± 0.05, suggesting moderate ovality of these structures. The dimensions of the strands were

characterized by histograms with a peak contour length of 20 ± 6 nm (n = 186; Fig. 2D) and a height of 0.4 ± 0.1 nm (n = 162; Fig. 2E). Based on the known polypeptide composition of pFXIII-A_2B_2, the observed molecular images could be interpreted as an A_2 globule with one or two individual thread-like B subunits.

The absolute values of heights of the A_2 globules and thread-like B subunits measured with AFM are smaller than the dimensions of the corresponding atomic structures of A_2 globules [36–38] and homologous sushi domains [52] determined using X-ray crystallography. This discrepancy of dimensions observed in the AFM images and full-atom crystal structures is likely to be a result of variable orientation possibilities of the FXIII-A_2 complex, as well as potential surface effects of GM-graphite and sample drying that affect the overall behavior of the molecule in AFM and may affect the measurements.

Structure of rFXIII-A_2—The rFXIII composed of two A subunits (ZymoGenetics) was visualized as globules with an average height of 3.7 ± 0.3 nm (n = 634; Fig. 3). The height value was close to the height of the globular portion of pFXIII-A_2B_2 (Table S1), so we concluded that in rFXIII each globule corresponded to an A_2 dimer, which is in agreement with the literature on the prevalent oligomeric state of free FXIII-A subunits [24,25,36]. A similar height value (3.3 ± 0.4 nm, n = 338) was obtained for the globular rFXIII-A_2 from Zedira, despite the presence of maltodextrin on the substrate that somewhat complicated the quantitative image analysis, because of the uneven background (Fig. S1, Table S1). An average circularity of rFXIII-A_2 molecules was equal to 0.91 ± 0.05 (n = 40). This value was significantly larger than the circularity of the globular cores of pFXIII molecules with two visible extensions (P < 0.005, Wilcoxon rank sum test). Thus, the shape of the globular portion of tetrameric pFXIII-A_2B_2 was slightly elongated compared to rFXIII-A_2.

Structure of rFXIII-B_2—rFXIII-B subunits were visualized as strands with an average contour length of 33 ± 3 nm (n = 175; Fig. 4A–C) and a height (thickness) of 0.6 ± 0.1 nm (n = 175; Fig. 4D). Importantly, not only was the contour length increased, but also the height of the strands was significantly greater compared to the thickness of the flexible strands observed in pFXIII-A_2B_2 (P < 0.001, Wilcoxon rank sum test; Table S1). The increased length of rFXIII-B subunits could be potentially attributed to either elongation resulting from dissociation of the monomeric B subunits from the A_2 dimer or to their dimerization. An additional argument for dimerization is an increase of thickness of B subunits separated from the A_2 globule (Table S1), suggesting that the separated rFXIII-B subunits exist in a dimeric form [40,53], whereas in the whole pFXIII-A_2B_2 tetrameric molecules the B subunits protrude from the globular portion of the protein as two disjointed single polypeptides.

Structural changes associated with activation of FXIII

To follow structural perturbations of FXIII during its activation, we compared the polypeptide chain compositions and AFM single-molecule images of pFXIII-A_2B_2 and rFXIII-A_2 before and after treatment with thrombin and Ca^{2+}. In addition, we imaged commercially available preactivated pFXIIIa.

Activation of pFXIII-A_2B_2—AFM samples of pFXIII prepared at a 30-min time-point of incubation with thrombin revealed that most of the B subunits dissociated from the globular portion of pFXIII (Fig. 5A,B) and appeared as free flexible strands with an average 33 ± 4 nm contour length (n = 148; Fig. 5D) and 0.6 ± 0.1 nm height (n = 148; Fig. 5E). These dimensions were significantly distinct from the corresponding parameters of the B subunit flexible strands seen in inactive pFXIII molecules that had a visible contour length of 20 ± 6 nm and a height of 0.4 ± 0.1 nm ($P < 0.001$ for both parameters, Wilcoxon rank sum test). These differences suggest that upon activation of pFXIII with thrombin in the presence of Ca^{2+}, B subunits dissociate from the A_2 dimer and self-associate to form B_2 dimers. We also measured the heights of globular particles remaining separated after 30-min activation of pFXIII (Fig. 5A–C). The height distribution (n = 327) was bimodal with two peaks: one at3.3 ± 0.6 nm corresponded to the whole tetrameric pFXIII-A_2B_2 and, potentially, dimeric FXIII-A_2, whereas the other peak at 2.1 ± 0.3 nm probably represented FXIII-A and/or FXIII-A* monomers. As a matter of fact, the number of globular particles in the AFM images reduced with increasing incubation time of pFXIII-A_2B_2 with thrombin: at 2 h after addition of thrombin, only a few globular particles were present. We attribute this effect to aggregation of the activated pFXIII previously observed by other researchers [29,32,54].

AFM of commercially available preactivated pFXIIIa also revealed the presence of monomeric A* subunits visualized as globules with an average height of2.5 ± 0.5 nm (n = 413; Fig. 6C), substantially smaller than the dimeric A_2 globules in pFXIII (Fig. 2C), as well as separated FXIII-B_2 dimers visualized as strands with a contour length of 36 ± 5 nm (n = 194; Fig. 6A–B,D) and a height of 0.6 ± 0.1 nm (n = 194; Fig. 6E). Intact pFXIII molecules were virtually missing in the preparation of preactivated pFXIIIa.

Activation of rFXIII-A_2—According to SDS-PAGE, at 30 min after treatment with thrombin and Ca^{2+}, about half of rFXIII-A_2 molecules were partially cleaved (Fig. 1C). In the AFM images of rFXIII-A_2 from ZymoGenetics activated for 30 min, we saw two types of globular particles: most of the particles had an average height of 2.0 ± 0.4 nm, corresponding to the monomeric A and/or A* subunits, whereas the minority had an average height of 3.4 ± 0.2 nm, corresponding to the intact dimeric rFXIII-A_2 (n = 439; Fig. 7). Similar results were obtained with activated rFXIII-A_2 from Zedira, namely the AFM images revealed small A and/or A* monomeric globules with an average height of 2.3 ± 0.4 nm (n = 540; Fig. S3).

Discussion

The crystal structures of FXIII-related molecules are limited to active monomeric and inactive dimeric A subunits without flexible B subunits [33,36–38]. Transmission electron microscopy of glutaraldehyde-crosslinked pFXIII-A_2B_2 did not allow for identification of individual subunits and did not reveal their spatial arrangement [39]. So, this work is aimed at providing structural information on various forms of individual molecules of FXIII and its subunits with an unprecedented resolution using single-molecule AFM. Our findings provide new information about the structural arrangement of inactive pFXIIIA_2B_2, as well as the changes in subunit composition following activation.

Tetrameric, dimeric and monomeric subunits of FXIII

Tetrameric pFXIII-A_2B_2—The inactive pFXIII exists in three structural variants, namely a globule with two, one or no thin flexible extensions. This structural diversity may reflect the equilibrium between association and dissociation of the B subunits from the A_2 dimer. Alternatively, the B subunits may be partially or fully wrapped around the globular A_2 dimer, making them invisible in AFM images. The first explanation is supported by the following calculation. Based on $K_d = 4.17 \times 9\ 10^{-10}$ M for A-B interactions [55] and FXIII concentration ~6.3 nM, in equilibrium 24% of A and B subunits dissociate, whereas 76% exist as a complex. According to our AFM data, 26% of the B subunits dissociate from the FXIII globular core, whereas 74% are connected to the globules, in excellent agreement with the calculated values.

Remarkably, two spread-out B subunits were typically both seen on one side of the globule, perhaps because FXIII-A_2 is asymmetrical and the B subunits might attach to asymmetrically positioned binding sites. Each of these binding sites is presumably located in the vicinity of the activation peptide [34] and includes critical amino acid residues Gly562 and Tyr283 [56]. This natural structural asymmetry might be even more pronounced in AFM because of a non-random preferential orientation of FXIII molecules during adsorption on the substrate.

rFXIII-A_2 homodimer—Although a crystallographic structure of FXIII-A_2 is available, its AFM imaging is important for identifying the A_2 dimer within inactive and activated pFXIII molecules. By AFM, rFXIII-A_2 is visualized as a globule with a size close to that of the pFXIII globular core (Fig. 3C, Fig. S2C), implying that the molecular dimensions of the globular portion of pFXIII are determined by the A_2 dimer and a contribution of B subunits is negligibly small.

Free B_2 homodimers and monomeric B subunits within pFXIII—Recombinant dimeric B subunits (rFXIII-B_2) appear as thin flexible strands with an average contour length of 33 nm, which is in good agreement with a 30-nm estimation obtained by transmission electron microscopy [39]. Because both the length and thickness (height) of the free B_2 dimers were significantly larger compared to the flexible strands protruding from the globular core of pFXIII-A_2B_2 molecules (Table S1), we conclude that these strands in pFXIII-A_2B_2 comprise monomeric B subunits. This deduction agrees with earlier studies showing that modified B subunits that are unable to dimerize with each other can still participate in formation of the A_2B_2 heterotetramer [40,53] if they possess intact sushi domains 1 and 2 [40,55].

Based on this reasoning, we can tentatively estimate how many sushi domains are seen in the single B subunits extending from the globular part of pFXIII and having a contour length of 20 nm in the AFM images (Fig. S5A). If the contour length of B_2 dimers (about 33 nm) corresponds to a previously suggested structural model, in which two B subunits have an antiparallel orientation as a result of inter-subunit interactions between sushi domains 4 and 9 [40], then the length of a B monomer should be about 27.5 nm (Fig. S5B). If that is true, then the 20-nm strands extending from the globular part of pFXIII molecules correspond to

seven or eight freely exposed sushi domains of the B subunit (Fig. S5A) and only sushi domains 1 and 2, which are critical for pFXIII heterotetramer formation, comprise the shorter portions of B subunits that are tightly bound to the globule formed by two A subunits and remain invisible [40,55].

FXIII-A monomers versus dimers—Our measurements strongly suggest that the oligomeric pFXIIIa-A_2B_2 and rFXIII-A_2 disassemble upon activation and form monomeric active A* subunits. In all four species of activated FXIII studied, the monomeric A or A* subunits were visualized as compact globules that were significantly smaller than A_2 dimers (~2.1 nm for a monomer vs. ~3.5 nm for a dimer, Table S1). To exclude the possibility that this difference in height was solely a result of spatial rearrangement of the A_2 dimers, we also calculated and compared the molecular volumes of these two types of globules. The 2.3-fold difference (185 ± 23 nm^3, $n = 20$, for a monomer, and 428 ± 58 nm^3, $n = 20$, for a dimer) strongly confirms that the observed variations in the height of A-subunit-containing globules reflect their monomeric vs. dimeric structure.

Structural mechanism of proteolytic activation of pFXIII

It has been generally accepted that activated pFXIIIa or cFXIIIa contain dimeric A* subunits (A^*_2) [29,31]. However, a few recent studies have suggested that the active A* subunits are monomeric and that their dissociation from dimers to monomers is an inherent part of FXIII activation [32–34]. Similarly, the existing data on the oligomeric vs. monomeric state of free B subunits are also controversial [23].

Our work provides direct evidence for the formation of monomeric FXIII-A* subunits and dimeric FXIII-B_2 subunits after activation (proteolytic cleavage of the activation peptide, AP) of pFXIII-A_2B_2 with thrombin and Ca^{2+}. This paradigm-changing concept is reflected by the equation:

$$A_2B_2 \xrightarrow{\text{Thr, Ca}^{2+}} 2A^* + B_2 + 2AP \quad (4)$$

It is conceivable that the conversion of A2B2 tetramer to A* monomers and B2 dimer can go through the intermediate heterodimeric complexes AA?, AB or A?B, although our experimental data do not provide evidence for that. In the samples prepared for AFM imaging 30 min after addition of thrombin and Ca2+ to pFXIII-A2B2 or rFXIII-A2, only about 1/2 of the A subunits were cleaved as judged from the SDS-PAGE (Fig. 1B–C). However, on the AFM images at this time-point of activation the vast majority of the A subunits were monomeric with very few A2 dimers, suggesting that cleavage of only one AP from the A2 dimer makes the two A subunits dissociate because the AA? (hetero)dimers are thermodynamically unstable in the presence of Ca2+. In the case of pFXIII-A2B2, dissociation of B subunits precedes separation of the AA? complex into monomeric A* and A subunits.

Importantly, in the circulation, binding of pFXIII to fibrinogen is mediated predominantly by the interaction between the B subunit of FXIII and the C-terminus of fibrinogen's gamma-

prime-chain [57]. Therefore, there is no conceivable spatial obstacle that would prevent dissociation of dimeric A* subunits into monomers upon activation of pFXIII that we observed in purified pFXIIIa.

Conclusions

In summary, our results provide single-molecule images that reflect conformational and orientational possibilities of the individual subunits of inactive and activated human plasma FXIII. Although the results of AFM depend on surface-related conditions that are different from solution and molecular dimensions are smaller from drying, they can capture fundamental structural features underlying the function of plasma-derived and cellular transglutaminases. Based on the AFM images, the inactive plasma FXIII (pFXIII-A_2B_2) consists of a globular A_2 dimeric core and two individual B subunits extending out from one side as flexible strands. The size of the globular part was found to be 3.5 nm and the extending filamentous strands were about 20 nm long. Recombinant inactive FXIII-A subunits in the absence of FXIII-B subunits were shown to form a globular homodimer about3.5 nm in size, recapitulating the structure of cellular FXIII. Recombinant FXIII-B subunits in the absence of FXIII-A subunits formed flexible homodimeric strands that were 0.6 nm thick and 33 nm long. The surface molecular topography revealed by AFM suggests that activation of pFXIII-A_2B_2 with thrombin and Ca^{2+} includes at least three concerted structural rearrangements: (i) dissociation of the initially monomeric B subunits from the globular core of the molecule; (ii) association of the released B subunits to form B_2 homodimers; and (iii) dissociation of the initially dimeric A subunits into enzymatically active monomers. Accordingly, activation of the B-subunit-free dimeric rFXIII-A_2 with thrombin and Ca^{2+} includes only one step, namely dissociation into monomeric enzymatically active A subunits.

Supplementary Material

Refer to Web version on PubMed Central for supplementary material.

Acknowledgements

We thank M. Maurer and B. Anokhin for providing rFXIII-A_2 (ZymoGenetics, USA). Funding was provided by NIH grants UO1-HL116330 and RO1-HL135254 and NSF grant DMR1505662, by a Scholar Award from the American Society of Hematology, and by the Program for Competitive Growth at Kazan Federal University.

References

1. Liu W, Jawerth JM, Sparks EA, Falvo MR, Hantagan RR, Superfine R, Lord ST, Guthold M. Fibrin fibers have extraordinary extensibility and elasticity. Science 2006; 313: 634. [PubMed: 16888133]
2. Helms CC, Ariens RAS, De Willige SU, Standeven KF, Guthold M. Alpha-alpha cross-links increase fibrin fiber elasticity and stiffness. Biophys J 2012; 102: 168–75. [PubMed: 22225811]
3. Houser JR, Hudson NE, Ping L, O'Brien ET, Superfine R, Lord ST, Falvo MR. Evidence that alphaC region is origin of low modulus, high extensibility, and strain stiffening in fibrin fibers. Biophys J 2010; 99: 3038–47. [PubMed: 21044602]
4. Collet J-P, Moen JL, Veklich YI, Gorkun OV, Lord ST, Montalescot G, Weisel JW. The alphaC domains of fibrinogen affect the structure of the fibrin clot, its physical properties, and its susceptibility to fibrinolysis. Blood 2005; 106: 3824–30. [PubMed: 16091450]

5. Ryan EA, Mockros LF, Weisel JW, Lorand L. Structural origins of fibrin clot rheology. Biophys J 1999; 77: 2813–26. [PubMed: 10545379]
6. Duval C, Allan P, Connell SDA, Ridger VC, Philippou H, Ariens RAS. Roles of fibrin alpha- and gamma-chain specific cross-linking by FXIIIa in fibrin structure and function. Thromb Haemost 2014; 111: 842–50. [PubMed: 24430058]
7. Piechocka IK, Kurniawan NA, Grimbergen J, Koopman J, Koenderink GH. Recombinant fibrinogen reveals the differential roles of α- and γ-chain cross-linking and molecular heterogeneity in fibrin clot strain-stiffening. J Thromb Haemost 2017; 15: 938–49. [PubMed: 28166607]
8. Standeven KF, Carter AM, Grant PJ, Weisel JW, Chernysh I, Masova L, Lord ST, Ariens RAS. Functional analysis of fibrin Gamma-chain cross-linking by activated factor XIII: Determination of a cross-linking pattern that maximizes clot stiffness. Blood 2007; 110: 902–7. [PubMed: 17435113]
9. Kurniawan NA, Grimbergen J, Koopman J, Koenderink GH. Factor XIII stiffens fibrin clots by causing fiber compaction. J Thromb Haemost 2014; 12: 1687–96. [PubMed: 25142383]
10. Aleman MM, Byrnes JR, Wang J-G, Tran R, Lam WA, Di Paola J, Mackman N, Degen JL, Flick MJ, Wolberg AS. Factor XIII activity mediates red blood cell retention in venous thrombi. J Clin Invest 2014; 124: 3590–600. [PubMed: 24983320]
11. Byrnes JR, Duval C, Wang Y, Hansen CE, Ahn B, Mooberry MJ, Clark MA, Johnsen JM, Lord ST, Lam WA, Meijers JCM, Ni H, Ariëns RAS, Wolberg AS. Factor XIIIa-dependent retention of red blood cells in clots is mediated by fibrin α-chain crosslinking. Blood 2015; 126: 1940–8. [PubMed: 26324704]
12. Cohen I, Gerrard JM, White JG. Ultrastructure of clots during isometric contraction. J Cell Biol 1982; 93: 775–87. [PubMed: 6889599]
13. Kasahara K, Souri M, Kaneda M, Miki T, Yamamoto N, Ichinose A. Impaired clot retraction in factor XIII A subunit – deficient mice. Blood 2010; 115: 1277–9. [PubMed: 19996413]
14. Rao KMK, Newcomb TF. Clot Retraction in a Factor XIII Free System. Scand J Haematol 1980; 24: 142–8. [PubMed: 7375813]
15. Tutwiler V, Litvinov RI, Lozhkin AP, Peshkova AD, Lebedeva T, Ataullakhanov FI, Spiller KL, Cines DB, Weisel JW. Kinetics and mechanics of clot contraction are governed by the molecular and cellular composition of the blood. Blood 2016; 127: 149–59. [PubMed: 26603837]
16. Kattula S, Byrnes JR, Martin SM, Holle LA, Cooley BC, Flick MJ, Wolberg AS. Factor XIII in plasma, but not in platelets, mediates red blood cell retention in clots and venous thrombus size in mice. Blood Adv 2018; 2: 25–35. [PubMed: 29344582]
17. Niewiarowski S, Markiewicz M, Nath N. Inhibition of the platelet-dependent fibrin retraction by the fibrin stabilizing factor (FSF, factor XIII). J Lab Clin Med 1973; 81: 641–50. [PubMed: 4698655]
18. Sakata Y, Aoki N. Cross-linking of alpha2-plasmin inhibitor to fibrin by fibrin-stabilizing factor. J Clin Invest 1980; 65: 290–7. [PubMed: 6444305]
19. Fraser SR, Booth NA, Mutch NJ. The antifibrinolytic function of factor XIII is exclusively expressed through α2-antiplasmin cross-linking. Blood 2011; 117: 6371–4. [PubMed: 21471521]
20. Valnickova Z, Enghild JJ. Human procarboxypeptidase U, or thrombin-activable fibrinolysis inhibitor, is a substrate for transglutaminases: Evidence for transglutaminase-catalyzed cross-linking to fibrin. J Biol Chem 1998; 273: 27220–4. [PubMed: 9765243]
21. Jensen PH, Lorand L, Ebbesen P, Gliemann J. Type-2 plasminogen-activator inhibitor is a substrate for trophoblast transglutaminase and Factor XIIIa Transglutaminase-catalyzed cross-linking to cellular and extracellular structures. Eur J Biochem 1993; 214: 141–6. [PubMed: 8099547]
22. Duckert F Documentation of plasma factor XIII deficiency in man. Ann N Y Acad Sci 1972; 202: 190–9. [PubMed: 4508922]
23. Muszbek L, Bereczky Z, Bagoly Z, Komaromi I, Katona E. Factor XIII: a coagulation factor with multiple plasmatic and cellular functions. Physiol Rev 2011; 91: 931–72. [PubMed: 21742792]
24. Schwartz ML, Pizzo SV, Hill RL, McKee PA. The subunit structures of human plasma and platelet factor XIII (fibrin-stabilizing factor). J Biol Chem 1971; 246: 5851–4. [PubMed: 5096097]
25. Schwartz ML, Pizzo SV, Hill RL, McKee PA. Factor XIII from plasma and platelets. J Biol Chem 1973; 248: 1395–407. [PubMed: 4405643]

26. Dorgalaleh A, Rashidpanah J. Blood coagulation factor XIII and factor XIII deficiency. Blood Rev 2016; 30: 461–75. [PubMed: 27344554]
27. Mitchell JL, Mutch NJ. Let's cross-link: diverse functions of the promiscuous cellular transglutaminase, factor XIII-A. J Thromb Haemost 2018; 17: 19–30.
28. Lorand L, Konishi K. Activation of the fibrin stabilizing factor of plasma by thrombin. Arch Biochem Biophys 1964; 105: 58–67. [PubMed: 14165504]
29. Chung SI, Lewis MS, Folk JE. Relationships of the catalytic properties of human plasma and platelet transglutaminases (activated blood coagulation factor XIII) to their subunit structures. J Biol Chem 1974; 249: 940–50. [PubMed: 4149557]
30. Yee VC, Pedersen LC, Bishop PD, Stenkamp RE, Teller DC. Structural evidence that the activation peptide is not released upon thrombin cleavage of factor XIII. Thromb Res 1995; 78: 389–97. [PubMed: 7660355]
31. Hornyak TJ, Shafer JA. Role of calcium ion in the generation of factor XIII activity. Biochemistry 1991; 30: 6175–82. [PubMed: 2059625]
32. Anokhin BA, Stribinskis V, Dean WL, Maurer MC. Activation of factor XIII is accompained by a change in oligomerization state. FEBS J 2017; 284: 3849–61. [PubMed: 28915348]
33. Stieler M, Weber J, Hils M, Kolb P, Heine A, Büchold C, Pasternack R, Klebe G. Structure of active coagulation factor-XIII triggered by calcium binding: Basis for the design of next-generation anticoagulants. Angew Chem Int Ed Engl 2013; 52: 11930–4. [PubMed: 24115223]
34. Gupta S, Biswas A, Akhter MS, Krettler C, Reinhart C, Dodt J, Reuter A, Philippou H, Ivaskevicius V, Oldenburg J. Revisiting the mechanism of coagulation factor XIII activation and regulation from a structure/functional perspective. Sci Rep 2016; 6: 30105. [PubMed: 27453290]
35. Muszbek L, Polgar J, Boda Z. Platelet factor XIII becomes active without the release of activation peptide during platelet activation. Thromb Haemost 1993; 69: 282–5. [PubMed: 8097064]
36. Yee VC, Pedersen LC, Le Trong I, Bishop PD, Stenkamp RE, Teller DC. Three-dimensional structure of a transglutaminase: human blood coagulation factor XIII. Proc Natl Acad Sci U S A 1994; 91: 7296–300. [PubMed: 7913750]
37. Fox BA, Yee VC, Pedersen LC, Le Trong I, Bishop PD, Stenkamp RE, Teller DC. Identification of the calcium binding site and a novel ytterbium site in blood coagulation factor XIII by X-ray crystallography. J Biol Chem 1999; 274: 4917–23. [PubMed: 9988734]
38. Weiss MS, Metzner HJ, Hilgenfeld R. Two non-proline cis peptide bonds may be important for factor XIII function. FEBS Lett 1998; 423: 291–6. [PubMed: 9515726]
39. Carrell NA, Erickson HP, McDonagh J. Electron microscopy and hydrodynamic properties of factor XIII subunits. J Biol Chem 1989; 264: 551–6. [PubMed: 2491853]
40. Souri M, Kaetsu H, Ichinose A. Sushi domains in the B subunit of factor XIII responsible for oligomer assembly. Biochemistry 2008; 47: 8656–64. [PubMed: 18652485]
41. Dong AC, Kendrick B, Kreilgard L, Matsuura J, Manning MC, Carpenter JF. Spectroscopic study of secondary structure and thermal denaturation of recombinant human factor XIII in aqueous solution. Arch Biochem Biophys 1997; 347: 213–20. [PubMed: 9367527]
42. Rinas U, Risse B, Jaenicke R, Abel K-J, Zettlmeissl G. Denaturation-renaturation og the fibrin-stabilizing factor XIII A-chain isolated from human placenta. Properties of the native and reconstituted protein. Biol Chem Hoppe Seyler 1990; 371: 49–56. [PubMed: 1969740]
43. Rosenfeld MA, Bychkova AV, Shchegolikhin AN, Leonova VB, Biryukova MI, Kostanova EA. Ozone-induced oxidative modification of plasma fibrin-stabilizing factor. Biochim Biophys Acta 2013; 1834: 2470–9. [PubMed: 23948453]
44. Protopopova AD, Litvinov RI, Galanakis DK, Nagaswami C, Barinov NA, Mukhitov AR, Klinov DV, Weisel JW. Morpho-metric characterization of fibrinogen's αC regions and their role in fibrin self-assembly and molecular organization. Nanoscale 2017; 9: 13707–16. [PubMed: 28884176]
45. Protopopova AD, Barinov NA, Zavyalova EG, Kopylov AM, Sergienko VI, Klinov DV. Visualization of fibrinogen αC regions and their arrangement during fibrin network formation by high-resolution AFM. J Thromb Haemost 2015; 13: 570–9. [PubMed: 25393591]
46. Loewy AG, Dunathan K, Kriel R, Wolfinger HL. Fibrinase: I. Purification of substrate and enzyme. J Biol Chem 1961; 236: 2625–33. [PubMed: 14466268]

47. Laemmli UK. Cleavage of structural proteins during the assembly of the head of bacteriophage T4. Nature 1970; 227: 680–5. [PubMed: 5432063]

48. Liu T, Qian W, Gritsenko MA, Ii DGC, Monroe ME, Moore RJ, Smith RD. Human plasma N-Glycoproteome analysis by immunoaffinity subtraction, hydrazide chemistry, and mass spectrometry. J Proteome Res 2005; 4: 2070–80. [PubMed: 16335952]

49. Kristiansen GK, Andersen MD. Reversible activation of cellular factor XIII by calcium. J Biol Chem 2011; 286: 9833–9. [PubMed: 21245142]

50. Lorand L, Gray AJ, Brown K, Credo RB, Curtis CG, Domanik RA, Stenberg P. Dissociation of the subunit structure of fibrin stabilizing factor during activation of the zymogen. Biochem Biophys Res Commun 1974; 56: 914–22. [PubMed: 4133182]

51. Klinov D, Dwir B, Kapon E, Borovok N, Molotsky T, Kotlyar A. High-resolution atomic force microscopy of duplex and triplex DNA molecules. Nanotechnology 2007; 18: 225102.

52. Aslam M, Perkins SJ. Folded-back solution structure of monomeric factor H of human complement by synchrotron X-ray and neutron scattering, analytical ultracentrifugation and constrained molecular modelling. J Mol Biol 2001; 309: 1117–38. [PubMed: 11399083]

53. Seelig GF, Folk JE. Noncatalytic subunits of human blood plasma coagulation factor. J Biol Chem 1980; 255: 8881–6. [PubMed: 7410400]

54. Cooke RD. Calcium-induced dissociation of human plasma factor XIII and the appearance of catalytic activity. Biochem J 1974; 141: 683–91. [PubMed: 4463958]

55. Katona É, Pénzes K, Csapó A, Fazakas F, Udvardy ML, Bagoly Z, Orosz ZZ, Muszbek L. Interaction of factor XIII subunits. Blood 2014; 123: 1757–63. [PubMed: 24408323]

56. Souri M, Ichinose A. Impaired protein folding, dimer formation, and heterotetramer assembly cause intra- and extracellular instability of a Y283C mutant of the A subunit for coagulation factor XIII. Biochemistry 2001; 40: 13413–20. [PubMed: 11695887]

57. Siebenlist KR, Meh DA, Mosesson MW. Plasma factor XIII binds specifically to fibrinogen molecules containing γ' chains. Biochemistry 1996; 35: 10448–53. [PubMed: 8756701]

Essentials

- Factor XIII is a heterotetramer with 2 catalytic A subunits and 2 non-catalytic B subunits.
- Structure of active and inactive factor XIII was studied with atomic force microscopy.
- Inactive factor XIII is made of an A_2 globule and 2 flexible B subunits extending from it.
- Activated factor XIII separates into a B_2 homodimer and 2 monomeric active A subunits.

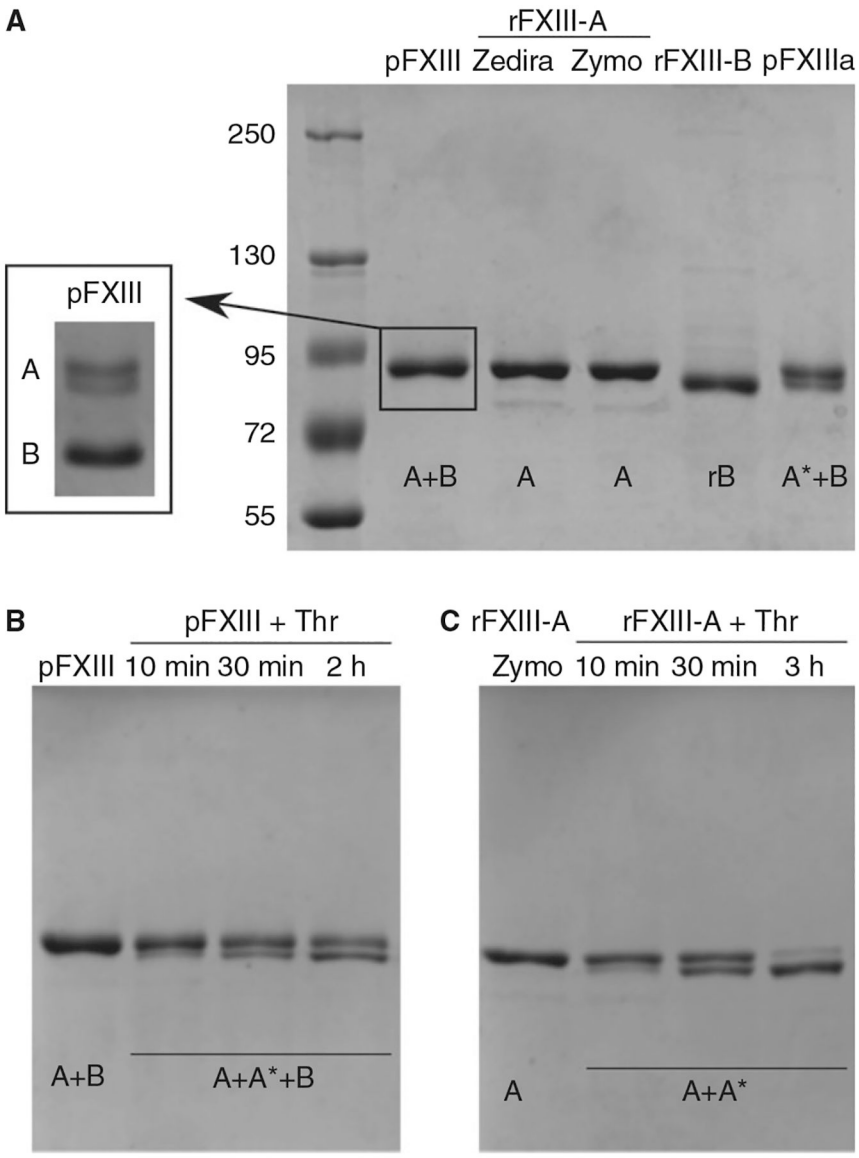

Fig. 1.

Polypeptide chain composition of plasma-purified (pFXIII) and recombinant (rFXIII) preparations of factor XIII. (A) SDS-PAGE in reducing conditions of the FXIII preparations used in this study. Lanes from left to right: molecular mass markers, pFXIII from Enzyme Research Laboratories containing A and B subunits, rFXIII-A subunits from Zedira, rFXIII-A subunits from ZymoGenetics, rFXIII-B subunits from Zedira, and preactivated pFXIIIa from Enzyme Research Laboratories. The insert shows an SDS-PAGE of pFXIII in non-reducing conditions. (B) Activation of pFXIII with thrombin and Ca^{2+} for 10 min, 30 min and 2 h. (C) Activation of rFXIII-A_2 (ZymoGenetics) with thrombin and Ca^{2+} for 10 min, 30 min and 3 h. Letters A, A*, B and rB at the bottom of the lanes indicate the subunit composition of each sample. All figures show entire gels.

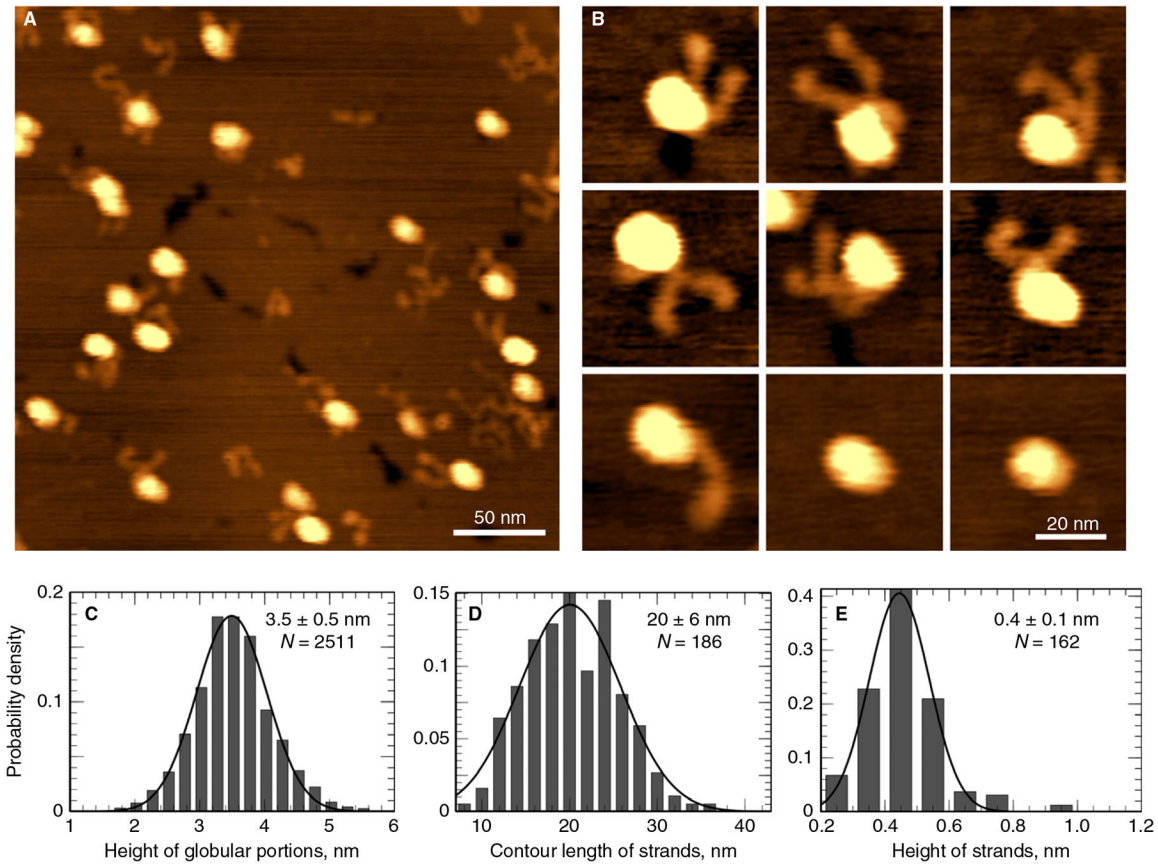

Fig. 2.

Atomic force microscopy (AFM) images and morphometric characterization of plasma-purified factor XIII (pFXIII) molecules. (A) A representative wide-field AFM image of pFXIII. (B) Individual pFXIII molecules showing characteristic structures with a globular portion and two strands. (C) A distribution of heights of the globular portions of the pFXIII molecules shown in A and B. (D) A distribution of contour lengths of the protrusions of strands of the pFXIII molecules shown in B. (E) A distribution of heights of the protrusions of strands of the pFXIII molecules shown in B.

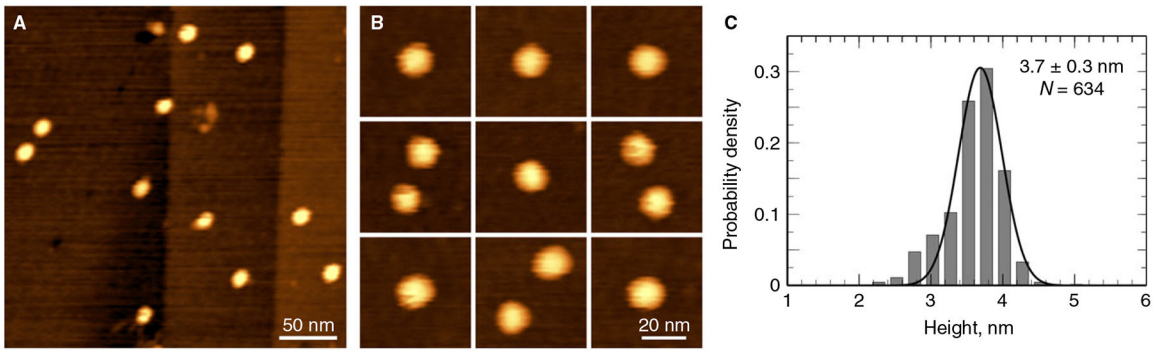

Fig. 3.

Atomic force microscopy (AFM) images and morphometric characterization of recombinant factor XIII -A_2 molecules (rFXIII-A_2). (A) A representative wide-field AFM image of rFXIII-A_2. (B) Individual rFXIII-A_2 molecules seen as globules. (C) A distribution of heights of the rFXIII-A_2 globules shown in A and B.

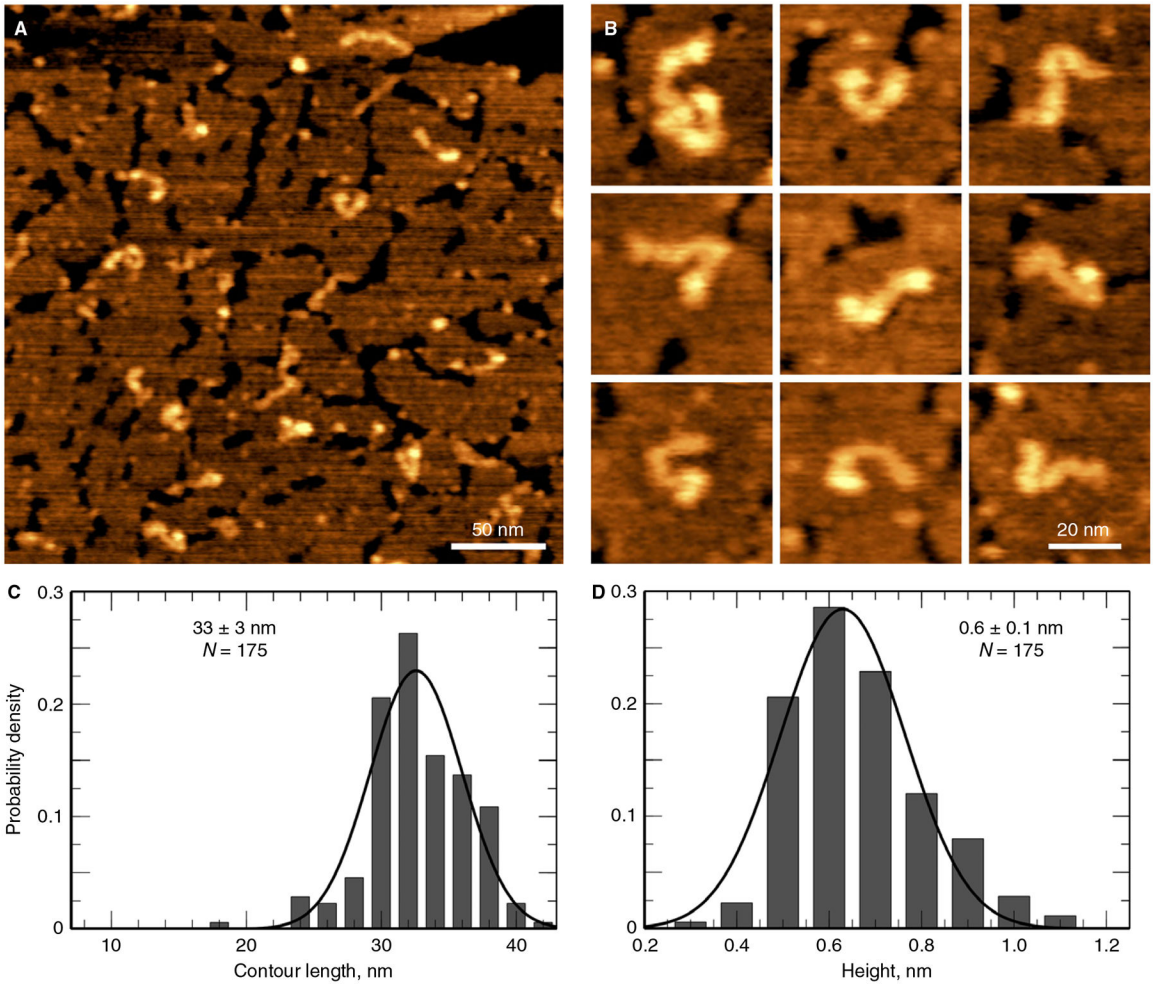

Fig. 4.

Atomic force microscopy (AFM) images and morphometric characterization of recombinant factor XIII-B_2 molecules (rFXIII-B_2). (A) A representative wide-field AFM image of rFXIII-B_2. (B) Individual rFXIII-B_2 molecules visualized as flexible strands. (C) A distribution of contour lengths of the rFXIII-B_2 strands shown in A and B. (D) Distribution of heights of the rFXIII-B_2 strands shown in A and B.

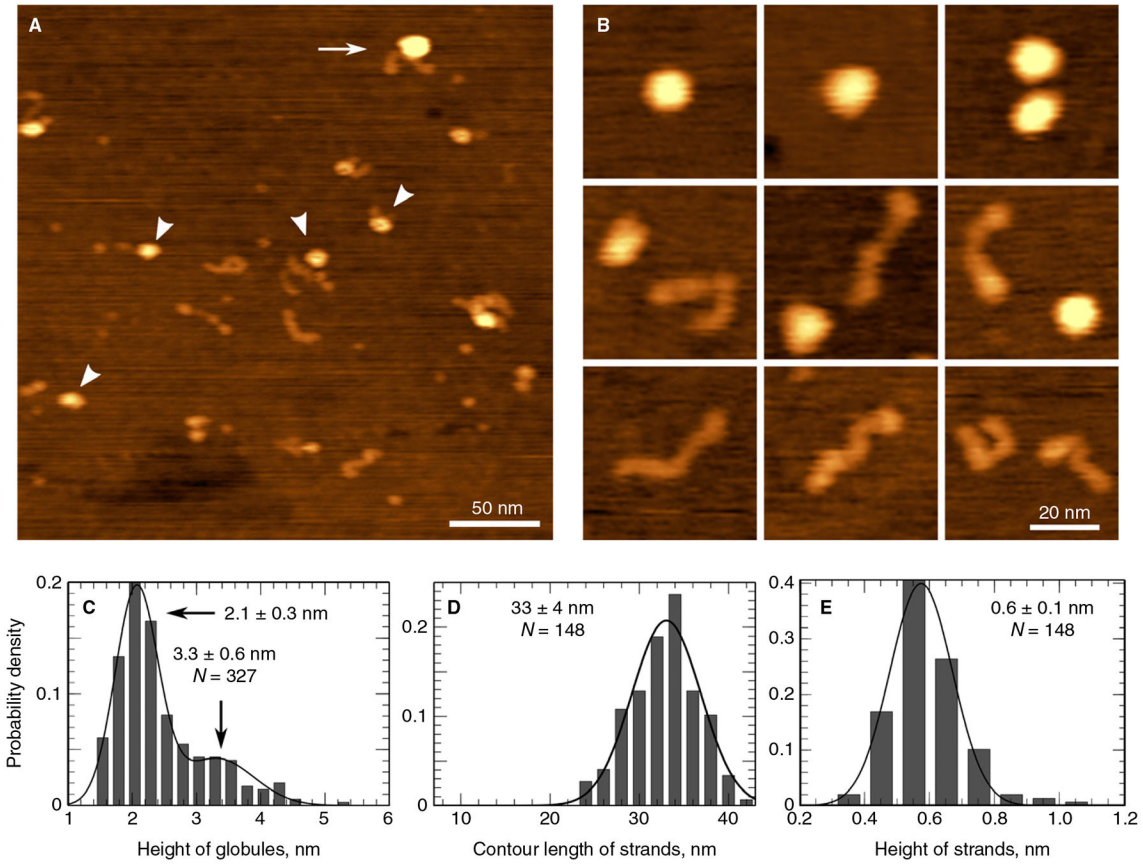

Fig. 5.

Atomic force microscopy (AFM) images and morphometric characterization of plasma-purified factor XIII (pFXIII) activated with thrombin and $CaCl_2$. (A) A representative image showing separation of globules and strands. Arrowheads point to activated (likely monomeric) A* and/or A subunits; an arrow points to an intact non-activated pFXIII molecule. (B) Individual pFXIII-A* (and/or pFXIII-A) subunits visualized as globules and pFXIII-B_2 dimers seen as strands. (C) A distribution of heights of the globules after activation of pFXIII shown in A and B. (D) Distribution of contour lengths of the strands formed after activation of pFXIII shown in A and B. (E) Distribution of heights of the strands formed after activation of pFXIII shown in A and B.

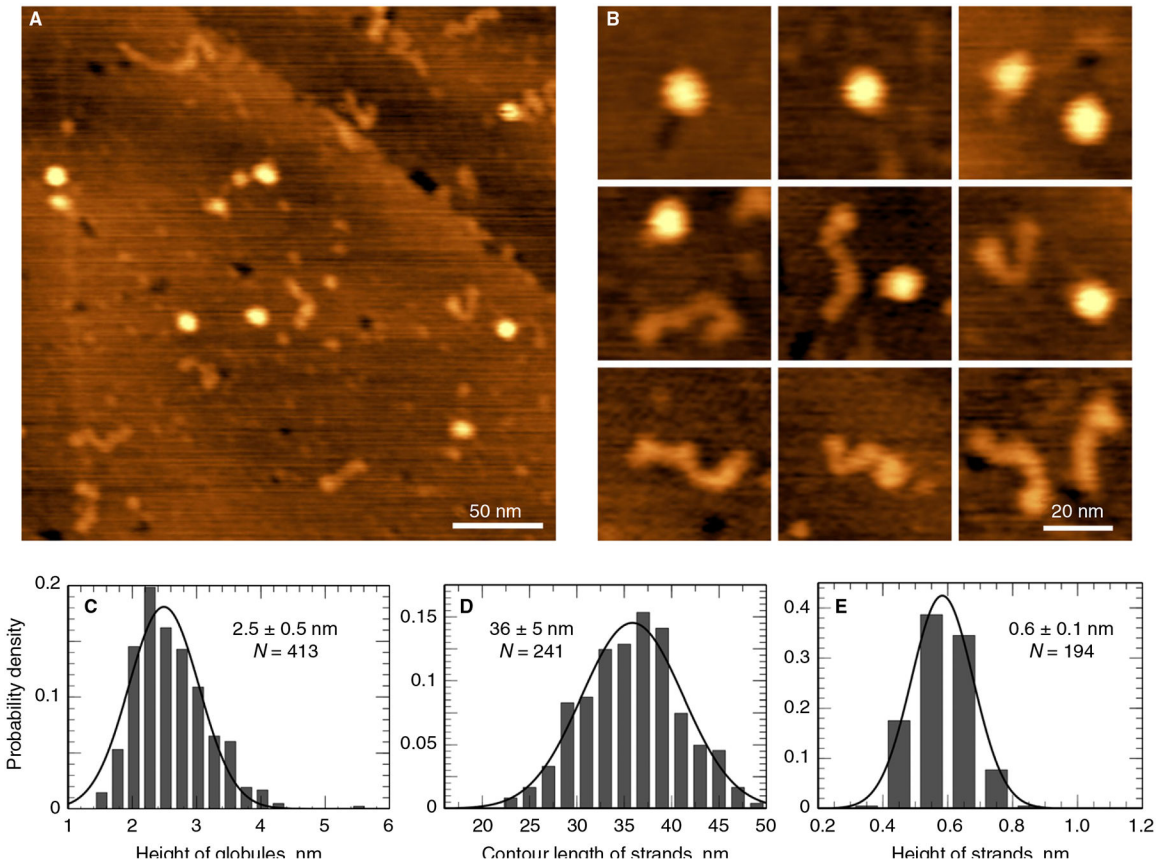

Fig. 6.

Atomic force microscopy (AFM) images and morphometric characterization of pre-activated plasma-purified factor XIII (pFXIIIa). (A) A representative image showing separate globules and strands. (B) Individual pFXIII-A* and/or A subunits visualized as globules and pFXIII-B_2 dimers visualized as strands. (C) A distribution of heights of the globules shown in A and B. (D) A distribution of contour lengths of the strands shown in A and B. (E) A distribution of heights of the strands shown in A and B.

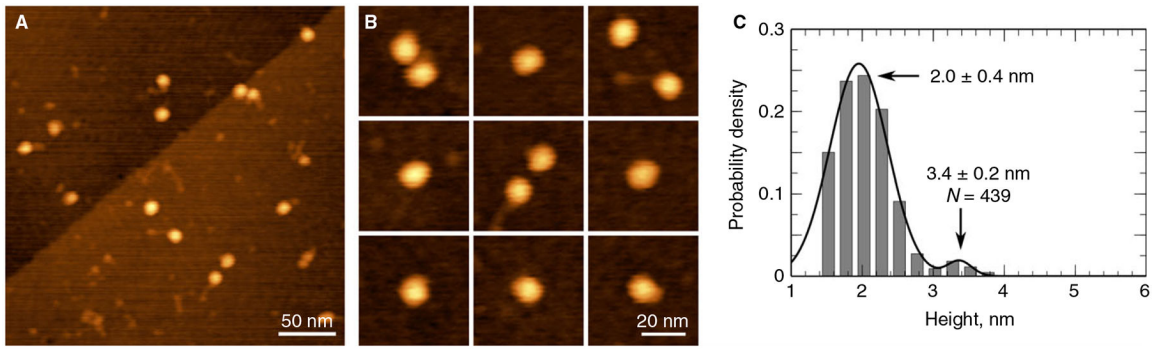

Fig. 7.

Atomic force microscopy (AFM) images and morphometric characterization of recombinant factor XIII-A_2 molecules (rFXIII-A_2) activated with thrombin and $CaCl_2$. (A) A representative image showing individual multiple small globules comprising monomeric A* and/or A subunits. (B) Individual monomeric A* and/or A subunits. (C) A distribution of heights of the globules shown in A and B.